UNIVERSITY OF THE
WITWATERSRAND,
JOHANNESBURG

SCHOOL OF MECHANICAL,
INDUSTRIAL & AERONAUTICAL
ENGINEERING

Solar Tracker Control Design

MECN4029A - Mechatronics II

Group 12

Ngwako Makudubela, 1611852 [100%]

Maruruwele Mokone, 2350229 [100%]

Mpumelelo Hlungwane, 2122606 [12%]

EXECUTIVE SUMMARY

A solar tracker controller for solar panels was designed to help students charge their devices during power cuts. The system's main components, the motor, and the panel, were mathematically modelled. Considering the power system requirements, performance specifications were outlined, forming a reference frame for the control design.

Performance analysis of the uncontrolled system indicated that control was necessary despite the stability shown by the Routh-Hurwitz method. Stability alone does not guarantee that the required performance specifications are met. Therefore, further analysis was undertaken to design a closed-loop system, ensuring that the output matches the input.

The control design process involved evaluating various controllers to ensure the performance specifications were met. Initially, a PI controller was considered sufficient due to the slow movement of the sun. However, the design of a controller depends on many factors, and no controller can be immediately disregarded. Ultimately, a PID controller was selected for the solar tracker due to its superior capability in accurately following the sun’s position.

The open loop transfer function obtained for the system was $\frac{0.0568}{s^3+10.568s^2+11.278s+55.682}$. The gain range was determined to be between -980 to 1118, ensuring the system operates within the desired performance specifications.

In summary, the design of the solar tracker controller involved a comprehensive analysis of the system's components and performance requirements. The PID controller was chosen for its effective tracking capabilities, ensuring that the solar panels can efficiently follow the sun's position to maximize energy capture and provide reliable power during outages.

TABLE OF CONTENTS

LIST OF FIGURES

LIST OF TABLES

NOMENCLATURE

θ	Angular displacement	rad
$\dot{\theta}$	Angular velocity	rad/s
$\ddot{\theta}$	Angular acceleration	rad/s^2
C	Damping factor	N/m
F_D	Drag force	N
F_L	Lift force	N
L	Inductor	H
r	Moment arm	m
R	Resistor	Ω
W	Weight	N

1 INTRODUCTION

1.1 Background and Information

A group of engineering students from the University of the Witwatersrand (Johannesburg) staying at the same building, decided to purchase a solar system as an alternative source of power during power cut-off. A power cut-off happens almost every day as their country, South Africa, experience power generation difficulties. As future engineers who like efficiency and optimization, their goal was to harness as much light as possible from the sun. Due to this goal, they decided to design a solar tracker system that would ensure they reach their intended goal. The 90 m high building that they stay in has an unused space at the rooftop where they plan to install the system.

1.2 Information Resources

Type of Solar Panel

Figure 1: A 100W Cinco solar panel [1].

The Solar panel Cinco 100W, has dimensions of 995x680x30mm and a weight of 10kg, with an output of 100W at 18.0V and 5.56A. It is made up of polycrystalline that ensures durability and efficiency. This, therefore, makes it a good choice for both residential and commercial applications [2].

Weather conditions in Johannesburg

In Johannesburg, the sun follows a path from east to west across the sky, while the prevailing wind direction is typically from the north. This is shown in the figure below that shows the average wind direction in South Africa per province.

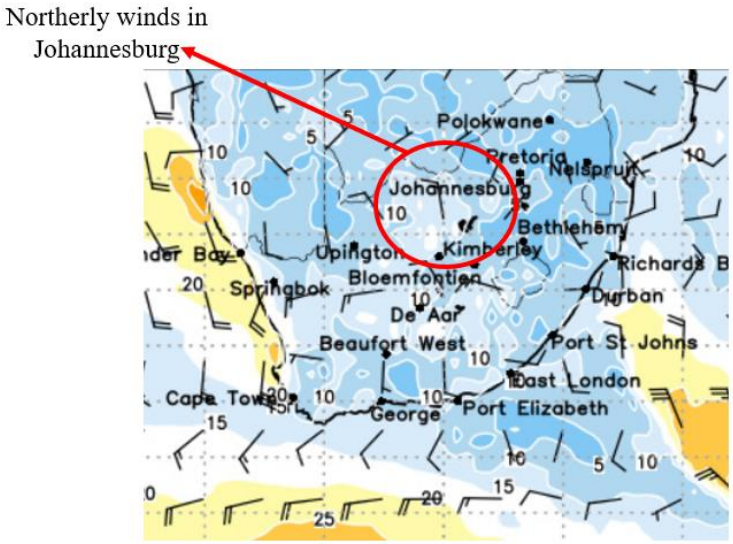

Figure 2 The average wind direction in Johannesburg [3].

The solar panel is firstly, oriented such that its azimuth remains fixed, aligned to optimize exposure to the sun's trajectory throughout the day. In this configuration, the panel faces the path of the sun as it moves from east to west. Given the northerly winds, the panel will experience aerodynamic forces that can affect its structural integrity and efficiency.

When considering the impact of wind on a solar panel, it's essential to account for both lift and drag forces. These forces arise due to the interaction between the wind and the panel's surface.

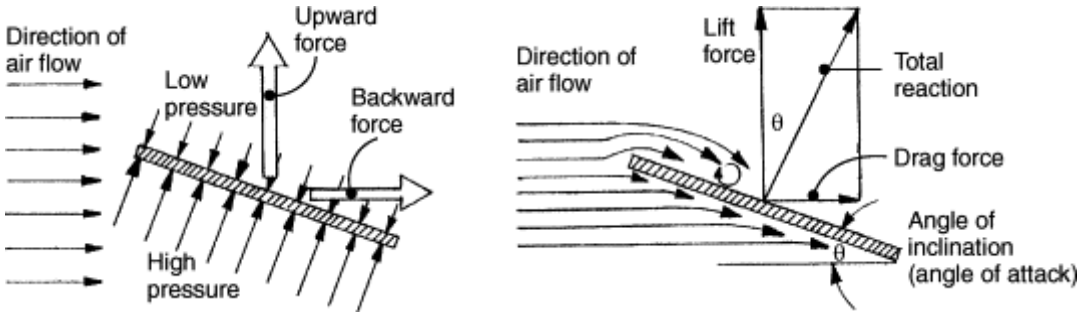

Figure 3 Lift and drag on a rectangular plate [4].

Lift and drag are the primary aerodynamic forces acting on the panel. Lift force is generated perpendicular to the wind direction and can cause upward or downward pressure on the panel, depending on its angle of incidence. Drag force, on the other hand, acts parallel to the wind direction, creating resistance that can lead to vibrations or structural stress.

Proper mounting and support structures must be in place to ensure the panel can withstand the lift and drag forces induced by the northerly winds, thereby maintaining optimal performance and longevity.

2 PERFOMANCE SPECIFICATIONS

Control design specifications are typically divided into two categories: time domain and frequency domain specifications. Time-domain specifications define lower and/or upper bounds for time response quantities such as first peak time, maximum peak time, rise time, maximum overshoot, and maximum undershoot, setting time, and steady-state error. Frequency-domain specifications are typically expressed as the resonant peak, phase margin, resonant frequency, and bandwidth [5].

2.1 Specifications in the Time Domain

Table 1. Performance specifications in the time domain

Specifications	Value
Maximum overshoot	20%
Peak time	< 2 s
Settling time	< 3 s
Rise time	$<$ 0.3 s
Decay ratio	≤ 0.3 s

2.2 Specifications in the Frequency Domain

Table 2. Performance specifications in the frequency domain

Specifications	Specification
Gain Margin	≥ 6 dB
Phase Margin	$\geq 30°$
Bandwidth	Wider

3 SYSTEMS MODELLING

3.1 Assumptions

The following assumptions were made to simplify the analysis of the system.

- The motor is connected to the solar panel in a gear ratio of 1:1. However, the equations used explicitly shows how the ratios are substituted in case different ratios need to be considered.
- The wind force generates drag and lift, which their resultant is parallel to point o, therefore not creating a torque about that point.
- The equations of motion were developed from a simplified 2D system and free body diagram.

3.1.1 Panel modelling

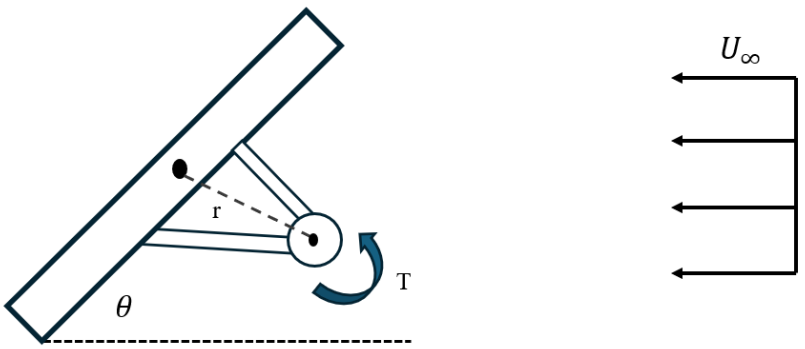

Figure 4. Panel side view with wind direction demonstration

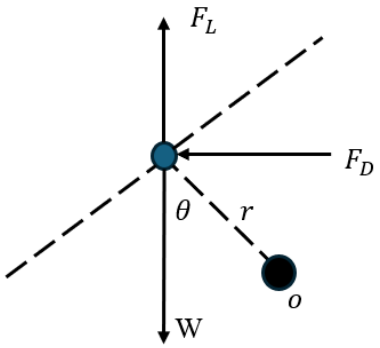

Figure 5. Free body diagram at centre of the panel around fixed-point O

Taking counterclockwise as positive,

$$\sum M_o = J\ddot{\theta} \tag{3.1}$$

$$T(t) - c\dot{\theta}(t) - Wr\sin\theta = J\ddot{\theta}(t) \tag{3.2}$$

Equation (3.2) is nonlinear due to the presence of the sine term. To linearize this term, small angle approximation was used. To prove validity of small angle approximations, Taylor Series was used, and the proof is shown below.

$$Let\ f(\theta) = \sin\theta \quad at\ point\ a = 0 \tag{3.3}$$

The linearized term would then look like Equation (3.4) according to Taylor Series

$$L(\theta) = f(a) + f'(a)(\theta - a) \tag{3.4}$$

$$f(0) = \sin(0) = 0 \tag{3.5}$$

$$f'(\theta) = \cos\theta \tag{3.6}$$

$$f'(0) = \cos(0) = 1 \tag{3.7}$$

$$\therefore L(\theta) = (0) + 1(\theta - 0) = \theta \tag{3.8}$$

Hence,

$$T(t) - c\dot{\theta}(t) - Wr\theta(t) = J\ddot{\theta}(t) \tag{3.9}$$

Taking Laplace of Equation (3.9) results in the following,

$$T(s) - cs\theta(s) - Wr\theta(s) = Js^2\theta(s) \tag{3.10}$$

Re-arrange Equation (3.10), then,

$$T(s) = Js^2\theta(s) + cs\theta(s) + Wr\theta(s) \tag{3.11}$$

Equation (3.11) describes the amount of torque required by the panel to rotate. This is essential as it aid in terms of the selection of the motor to be used. At this point, the J refer to the inertia of the panel only.

3.1.2 Motor integrated with panel modelling

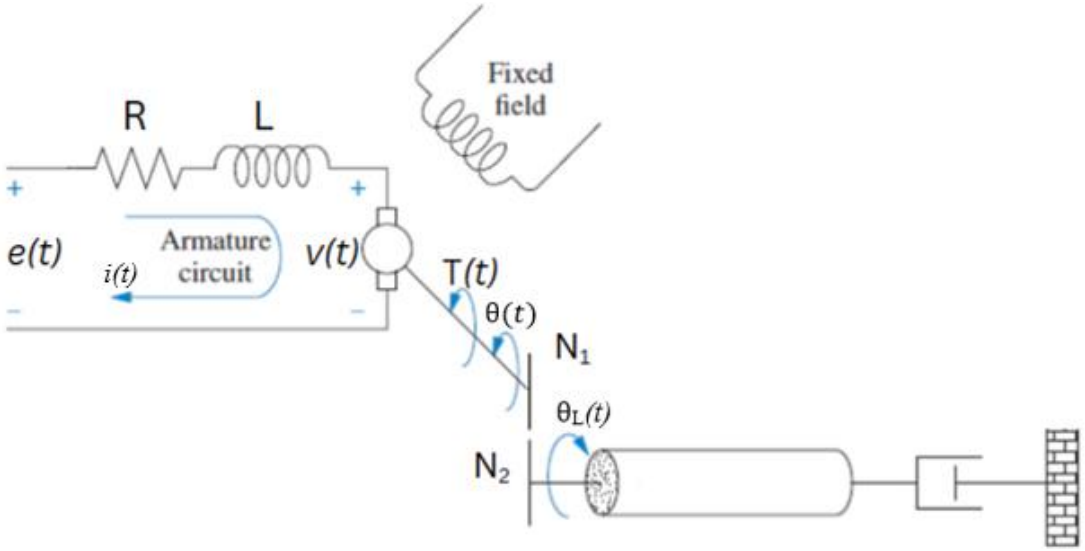

Figure 6: The electromechanical representation of the motor and the panel.

$$v(t) = K_b\dot{\theta} \tag{3.12}$$

Taking the Laplace transform of Equation (3.13), we get the following.

$$V(s) = K_b s\theta(s) \tag{3.13}$$

Using Kirchhoff's voltage law, Equation (3.14) below was derived.

$$Ri(t) + L\frac{di(t)}{dt} + v(t) = e(t) \tag{3.14}$$

Taking the Laplace transform of Equation (3.14), the equation below follows

$$RI(s) + LsI(s) + V(s) = E(s) \tag{3.15}$$

The torque developed by the motor is proportional to the armature current, writing it in a Laplace transformed way gives.

$$T(s) = K_t I \tag{3.16}$$

Where K_t is a constant of proportionality and is referred to as motor torque constant

$$I(s) = \frac{1}{K_t} T(s) \tag{3.17}$$

Substituting Equation (3.13) and (3.17) into Equation (3.15) yields

$$\frac{(R + Ls)T(s)}{K_t} + K_b s\theta(s) = E(s) \tag{3.18}$$

Rearranging,

$$T(s) = \frac{[E(s) - K_b s\theta(s)]K_t}{(R + Ls)} \tag{3.19}$$

For this analysis, the assumption of a unit gear ratio was made. This means the amount of torque require by the panel would be the same as that delivered by the motor, as well as $\theta(s)$ of the motor and panel, hence Equations (3.11) and (3.19) can be equated to yield Equation (3.20) below.

$$\frac{[E(s) - K_b s\theta(s)]K_t}{(R + Ls)} = Js^2\theta(s) + cs\theta(s) + Wr\theta(s) \tag{3.20}$$

Simplifying to get the transfer function in terms of input and output yields,

$$\frac{\theta(s)}{E(s)} = \frac{K_t}{[(R + Ls)(Js^2 + cs + Wr) + (K_b K_t)]} \tag{3.21}$$

Expanding the denominator,

$$\frac{\theta(s)}{E(s)} = \frac{K_t}{(LJ)s^3 + (RJ + cL)s^2 + (LWr + cR + K_b K_t)s + WrR} \tag{3.22}$$

Simplifying further to get a unit coefficient of s^3,

$$\frac{\theta(s)}{E(s)} = \frac{\frac{K_t}{LJ}}{s^3 + (\frac{RJ + cL}{LJ})s^2 + \left(\frac{LWr + cR + K_b K_t}{LJ}\right)s + \frac{WrR}{LJ}} \tag{3.25}$$

Note the nomenclature of the parameters at this point.

$$J = J_m + J_L(\frac{n_1}{n_2})^2 \quad (3.23)$$

$$C = C_m + C_L(\frac{n_1}{n_2})^2 \quad (3.24)$$

J – equivalent inertia, J_m – motor inertia, J_L – panel inertia, $\frac{n_1}{n_2}$ - gear 1 and 2 ratios, C - equivalent damping factor, C_m – damping factor of the motor and C_L – damping factor of the panel.

3.2 System Parameters

The specifications to be used in this assignment are summarised in the table below.

Table 3: Specifications for the motor and solar panel [6].

Motor Specifications	
Torque Constant [V.s/rad]	0.5
Back emf constant [N.m/A]	0.5
Armature resistance[Ω]	10
Mass moment of Inertia[kg.m2]	1.2
Dampening constant [N.m.s/rad]	5
Gear Ratio	1
Solar Panel Specifications	
Mass[kg]	5
Dimensions [mm]	995 x 680 x 30
Moment arm, r [m]	0.1
Moment of Inertia[kg.m2]	7.6

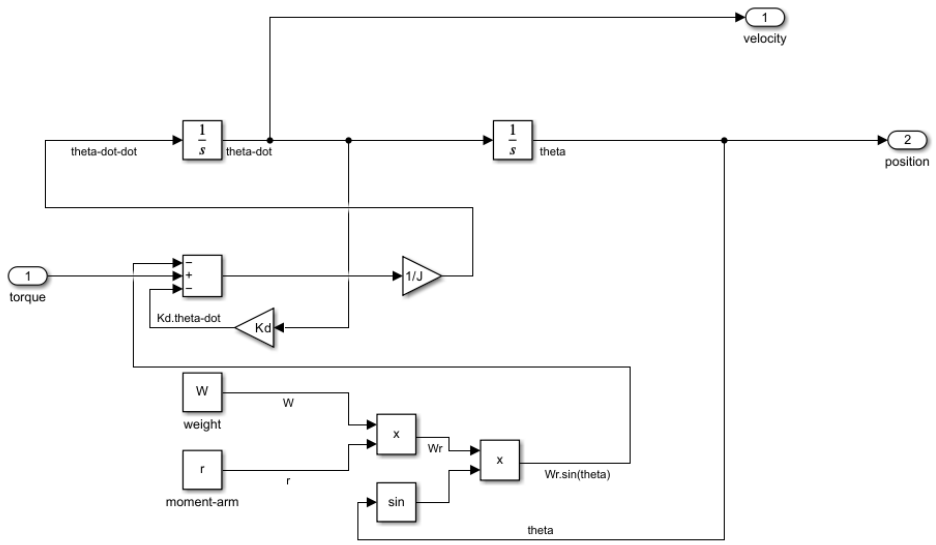

Figure 7. Block diagram for the nonlinear solar panel model.

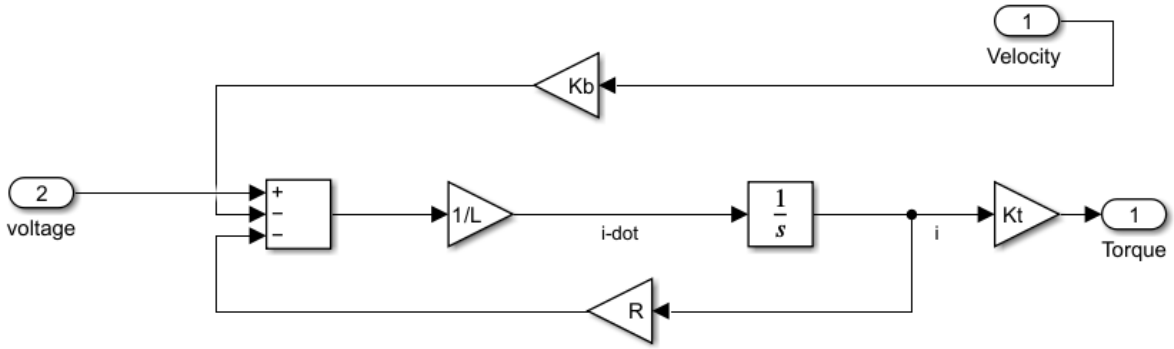

Figure 8. Motor block diagram for the motor used.

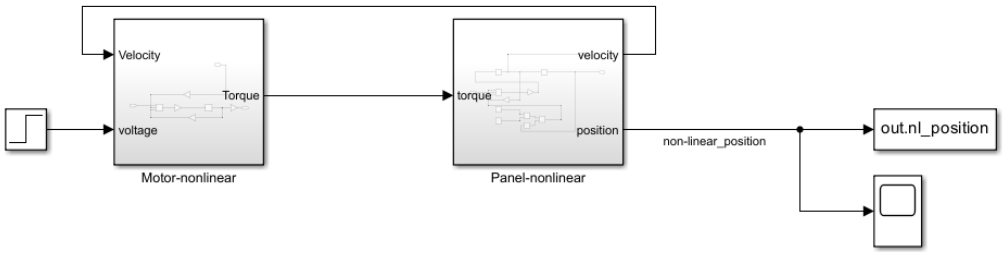

Figure 9. Block diagram for the nonlinear model

4 PERFOMANCE ANALYSIS: UNCONTROLLED PLANT

Analysis where the basic performance of the uncontrolled systems both in time and frequency domains was undertaken and this section intends to report on it. Most importantly, comparison of time-responses of the linear and nonlinear models of systems was processed. This processing was done with in Simulink, and it included the use of input signals that are as close to reality as possible. The inputs considered were step, ramp, and sine wave.

4.1 Time Domain Analysis

The figures to follow in this section provide a comparison of the uncontrolled systems, both linear and non-linear, according to time and position of the solar panel. Input signals were used to see the behavior of these systems when no control is implemented.

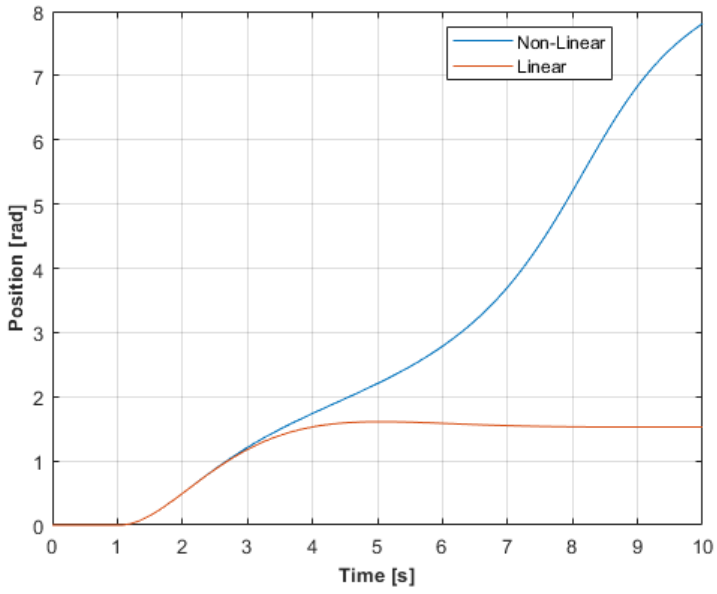

Figure 10. Uncontrolled system response with unit step input

Figure above shows uncontrolled system response of both linear and non-linear model due to a unit step input. Notice from the figure that both responses do not lie anywhere around 1 rad, which is the unit step. Furthermore, it is evident that comparing linear and non-linear responses,

the linear response seemed to better align with the input as compared to the non-linear response. The deviation between these responses came because of the sine function that differentiates them, which when linearized led to the linear model.

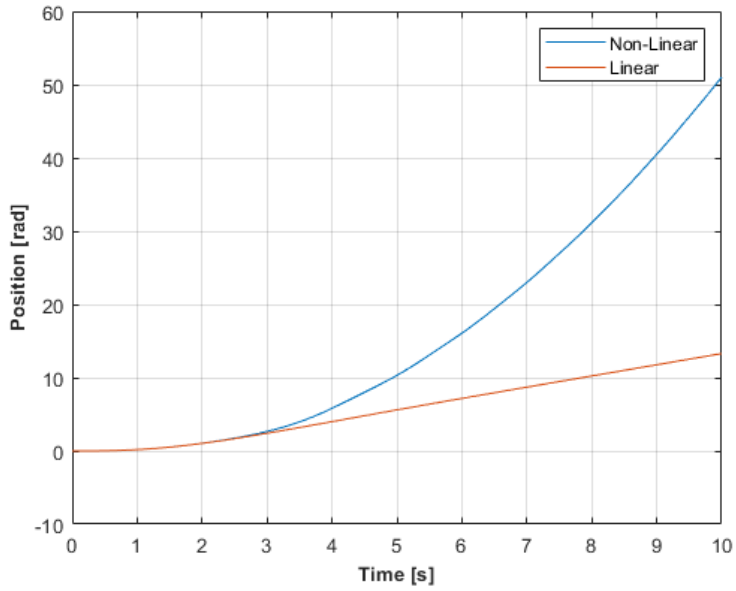

Figure 11. Uncontrolled system response with unit ramp input

The above figure is evidence of the different responses of both linear and non-linear systems from a unit ramp input. As seen from Figure 11, both responses remain the same for a period of about 2.5 s and thereafter the non-linear response diverges further away from the linear one.

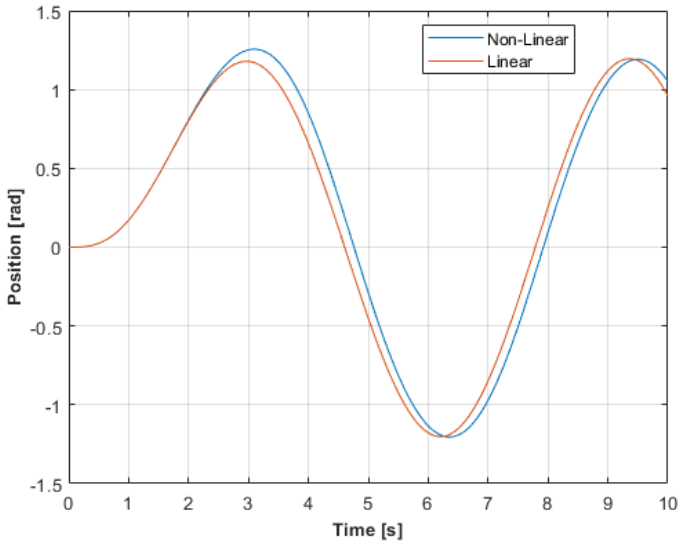

Figure 12. Uncontrolled system response with unit amplitude sine wave

The above figure provides evidence of the different responses for both linear and nonlinear. This response is due to a unit amplitude sine wave excitation. As seen in Figure 12, both responses remain the same for a period of about 2.5 s and thereafter, the nonlinear response diverges further away from the linear one. This is to say the behaviour of the nonlinear response is more chaotic as compared to the linear one.

4.2 Frequency Domain Analysis

Bode plot shows the frequency response of a system. It shows how magnitude and phase of the transfer function change with frequency. The magnitude plot shows the logarithmic (in decibels) of the transfer function with frequency (also in logarithmic scale).

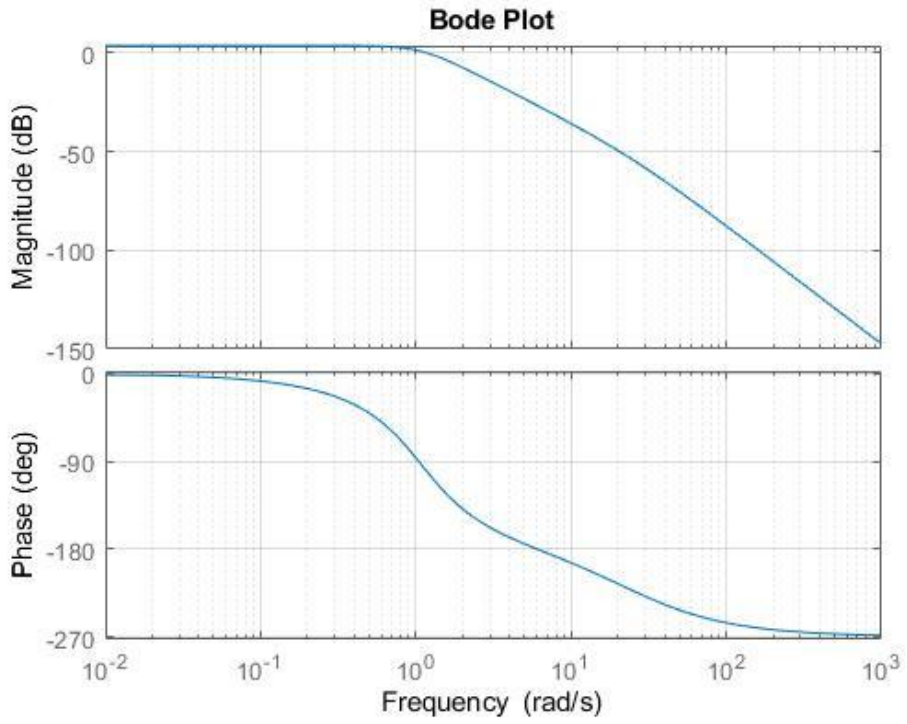

Figure 13: The bode plot for the linear system.

From the magnitude plot, the following can be deduced:

- At low frequency, the magnitude plot is constant which indicates that the system has constant gain.
- At high frequency, the slope drops for each pole in the transfer function.

Similarly, on the phase plot, it can be observed that:

- At low frequency, the phase shift is low indicating that both input and output signals are in phase.
- At high frequency, the phase shifts by decreasing. For a first and second order systems, the phase was expected to shift to -90 and -180 consecutively. Since the system considered in this case is a third order, it was well expected that the phase shifts to -270.

5 STABILITY ANALYSIS: UNCONTROLLED PLANT

The stability of a system can either be stable, unstable, or marginally stable. The system response is approaches zero as time goes to infinity when it is stable; grows without bound when unstable and is constant or oscillates when it is marginally stable [7]. To make accurate stability predictions, the closed-loop system differential equation should be at least third order [8].

The transfer function of the open loop system (obtained from the modelling of the panel and the motor) is,

$$\frac{\theta(s)}{E(s)} = \frac{0.0568}{s^3 + 10.568s^2 + 11.278s + 55.682} \quad (5.1)$$

5.1 Linear Model Stability

The linearized transfer function was used to test for stability in this section.

5.1.1 Routh Hurwitz Method

The characteristic equation for the system is obtained when the denominator is equated to zero.

$$s^3 + 10.568s^2 + 11.278s + 55.682 = 0 \quad (5.2)$$

The characteristic equation satisfies both the necessary conditions for stability, which are,

- All the coefficients of the equation should have the sign and
- None of the coefficients vanishes (i.e. there is $s^n, s^{n-1}, \dots, s^0$)

To further test that the system is stable, the Routh array was used to test for stability. This method allows to test for stability without finding the roots of the system.

Table 4: A Routh Array for the open loop system.

s^3	1	11.278
s^2	10.568	55.682
s^1	6	0
s^0	55.682	0

The number of sign changes = 0. This means that the system is stable and as there are no poles in the Right-Half Plane (RHP).

5.1.2 Nyquist

The number of closed-loop poles in the right half-plane can be determined using the Nyquist criterion.

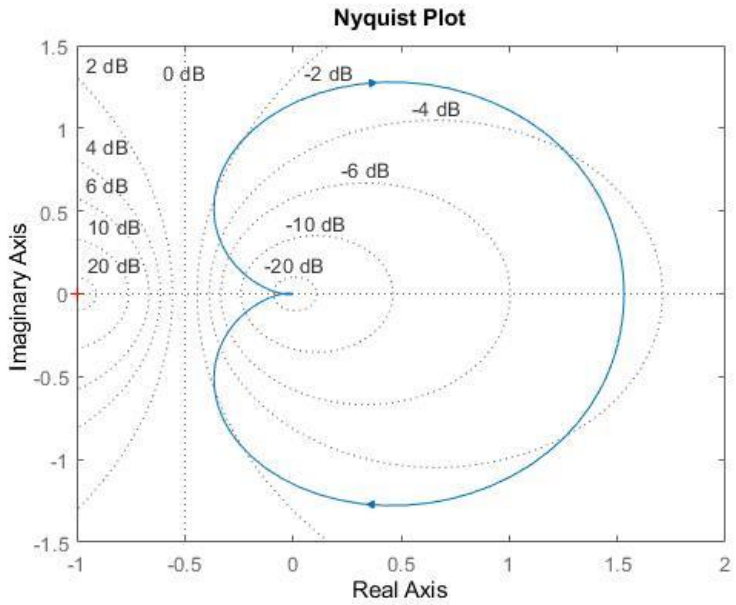

Figure 14: The Nyquist plot for the linear system.

The gain margin is the amount by which the system gain can be increased before the system reaches the verge of instability.

$$-\frac{1}{a} = -0.045$$

$$G_M = 20 \log a$$

$$G_M = 26.94\ dB$$

With a gain margin of 26.94 dB, the system can withstand a gain rise of around 22.22 (because a = 22.22 dB) before becoming unstable, suggesting strong resilience against gain variations.

5.1.3 Pole Zero Map

The roots of the linear transfer function are:

$s_1 = -10$

$s_{2,3} = -0.285 \pm i2.343$

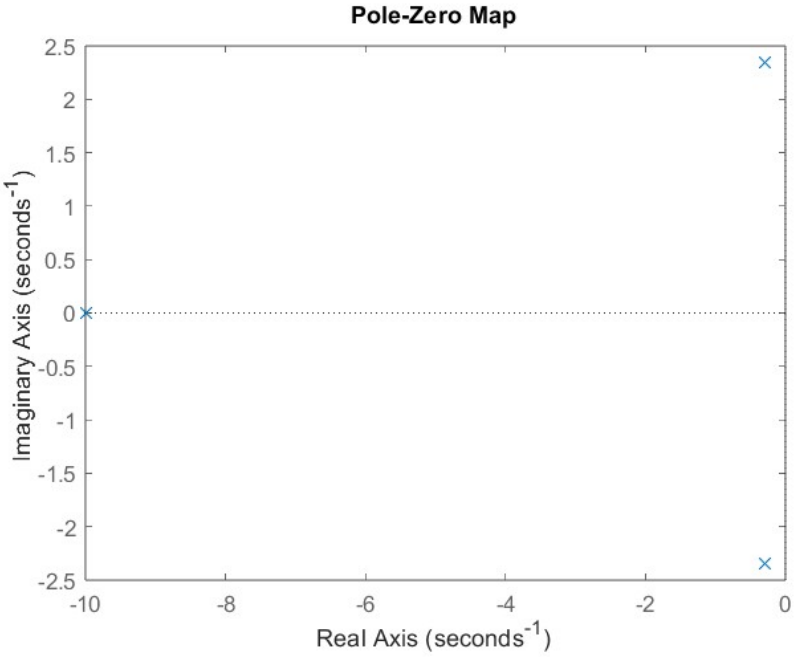

Figure 15: The Pole-Zero plot of the linearized model.

The pole-zero plot depicts the transfer function's poles and zeroes in the complex plane. The Poles are shown by 'x' markers, and they highlight the places at which the transfer function approaches infinity. The position of these poles has a significant impact on the system's stability and dynamics. In the above Figure, the poles are at (-10, 0), (-0.285 + 2.343i), and (-0.285 – 2.343i).

Zeros are represented by 'o' markers and show the sites at which the transfer function equals zero. They can impact the system's frequency response but have effect on stability. In this case there are no zeros in the transfer function.

5.2 Non-Linear Model Stability

The specifications of the motor given in the prior sections correspond to a motor that can generate a torque of 5 N.m. The nonlinear differential equation used is:

$$J\frac{d^2\theta}{dt^2} + c\frac{d\theta}{dt} + Wrsin\,\theta = T(t) \qquad (5.3)$$

5.2.1 Bounded Input Bounded Output (BIBO)

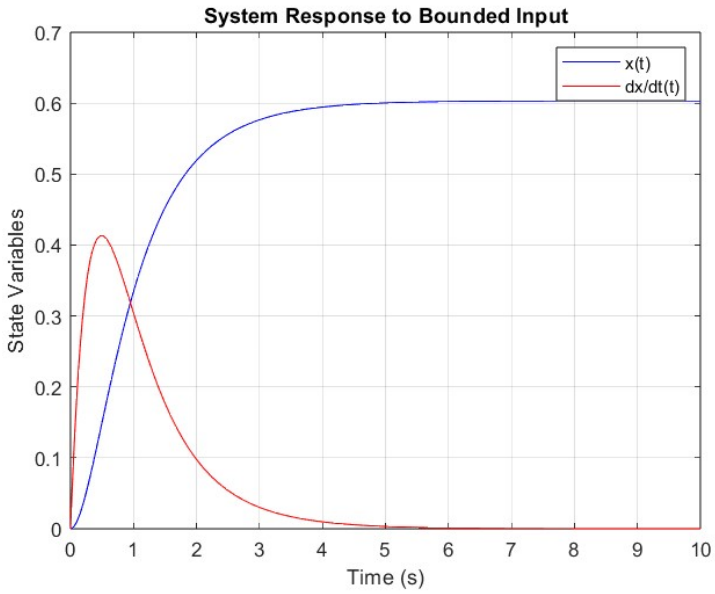

Figure 16 BIBO stability for the nonlinear system.

The system does not diverges\s to infinity when time goes to infinity. This implies that the nonlinear system is BIBO stable. It responds with bounded outputs for bounded inputs. When the difference between the velocity and position graph is less than ± 10, the system is stable.

6 CLOSED LOOP CONTROLLER DESIGN

6.1 Root-Locus

Root locus, which is a graphical presentation of the closed-loop poles as a system parameter is changed. This method was used to represent the state of the system in consideration.

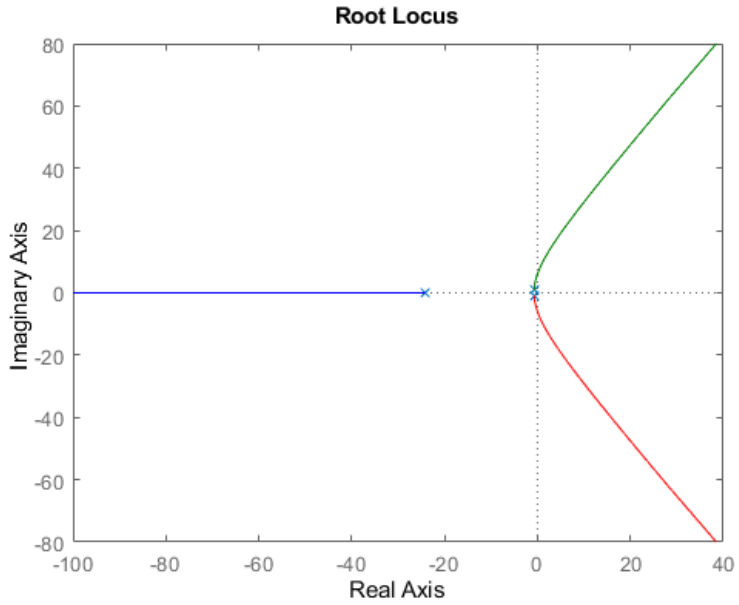

Figure 17 The system root locus.

6.2 Proportional-Integral-Derivative (PID)

When control was being designed, real sun position data was considered as the gains obtained from the controller would have to align with the input. It was evident from the uncontrolled plant that control would be required. As a result, P, I, PI and PID were tuned to find the controller that would best suit the application at hand.

An attempt to analytically determine the gain value K_P was made. This was not successful since the plant transfer function was not in the form that would allow for determination of the gain. To determine this gain, the plant transfer function would have to be in the form shown in

Equation (6.1). However, since the transfer function had an additional constant, other methods were required to determine the gain value.

$$G_P = \frac{{w_n}^2}{s^2 + 2\zeta w_n s + {w_n}^2} \qquad 6.1$$

Due to the transfer function being in a different form, this meant it would be difficult to obtain subsequent gain values (K_I and K_D). Methods such as the root locus were used, however this method does not specifically give the gain value. While the gains were not determined analytically, they were tuned and simulated in Simulink to see which control would best be suited for the solar panel tracker.

Comparison of the controllers was made for both linear and nonlinear systems and the results are shown below:

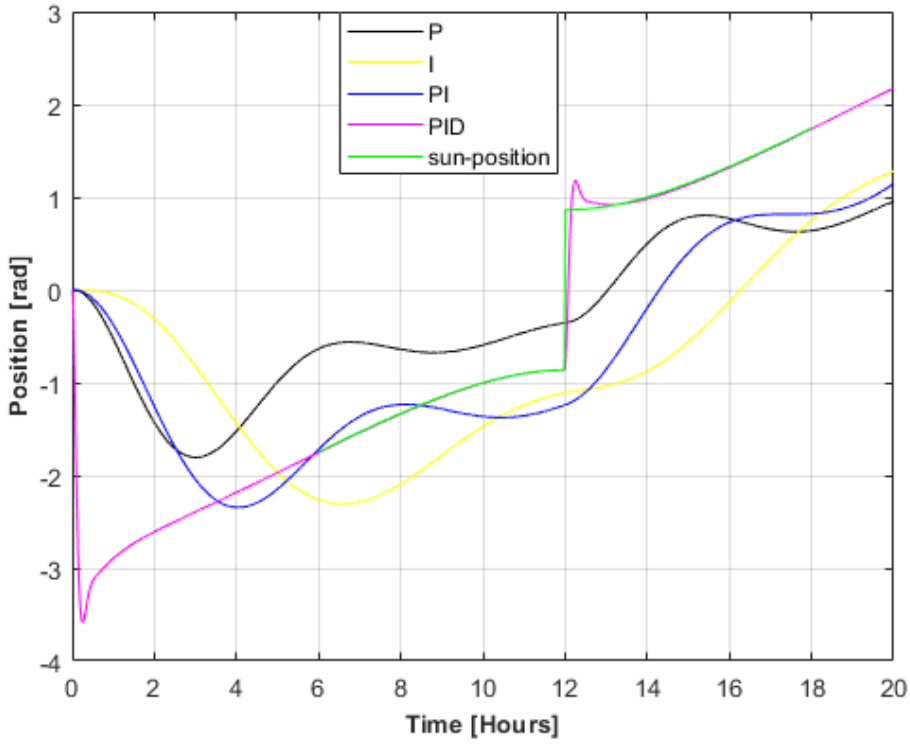

Figure 18. Controller comparison relative to sun's position in summer (day 355).

As seen from Figure 18 above, the only controller that can best follow the sun's position is the PID. The effective tracking starts from the sixth hour until the eighteenth hour. The PI controller was expected to be sufficient since the sun does not change direction quickly. However, the results show that even the derivative controller, which cannot be used alone, was necessary. Tuning was done in Simulink to obtain the most suitable values for the outlined performance specification.

While the PID follows the sun's position more accurate than the other controllers, it also has its shortcomings since it does not perfectly reflect the sun's position. These shortcomings were already taken into consideration by imposing the performance specifications. Taking a close look at the PID's response just after 12, it is evident that the controller had to readjust to continue following the sun's position. Around 12, the sun would reach it maximum angle and from there start declining. This explains the reason for the need to readjust.

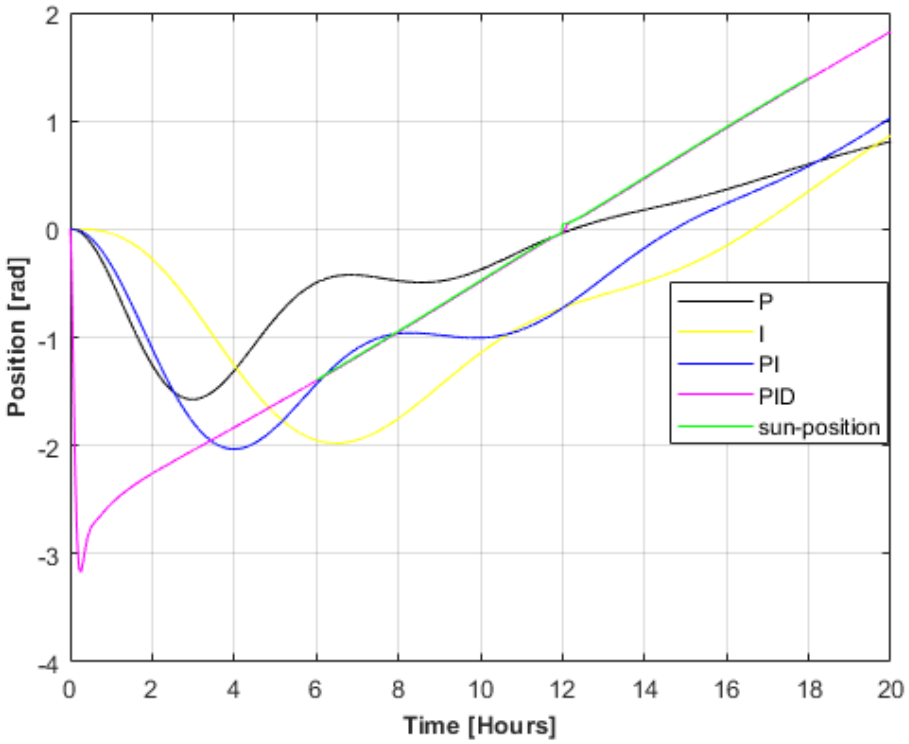

Figure 19. Controller comparison relative to sun's position in winter (day 173).

Similarly, it is evident from Figure 19 above that PID controller would be applicable in both summer and winter. As such this would be a viable controller to use for the solar panel tracker. Interesting points to note are that some of the controllers were totally not going to work in that they do not even at a single state interact with the sun's position. Notice how in this figure the I-controller alone never align with the sun's position. This controller uses integrator to eliminate steady state error. Since it does not interact at any point with the sun's position, this is not to say there is no steady state error but simply mean the controller alone is not adequate to eliminate the error.

While the linearized model provides sufficient proof that the nonlinear model can also track the sun's position, efforts were made to also give an illustration of how the panel responds in a nonlinear model.

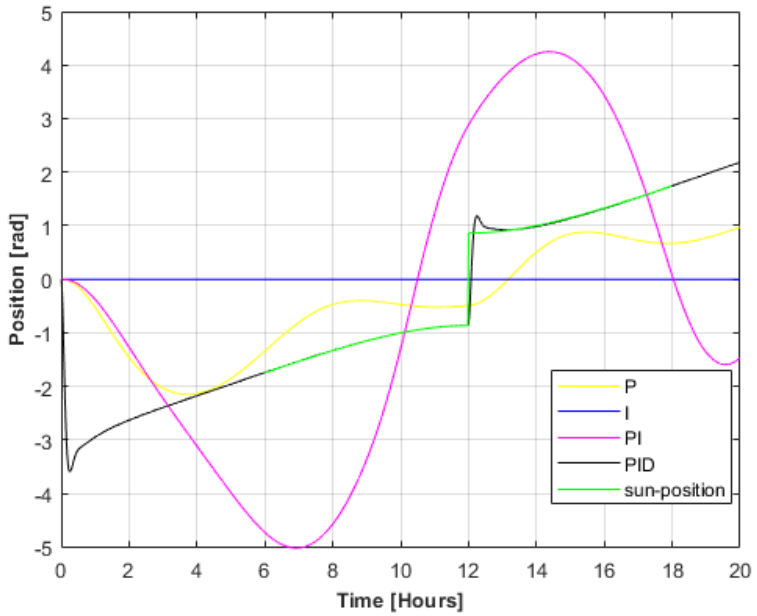

Figure 20. Controller comparison for nonlinear system in summer (day 355).

Notice how the PID controller follows the sun's position even for nonlinear model. This is just proof that if the nonlinear model was correctly linearized, great insights in terms of what type of control would be required for model can be extracted. Recall that the integrator controller was said to be the least controller to follow the sun's path. This is still evident in the nonlinear model; hence this are the kind of insight that can be extracted.

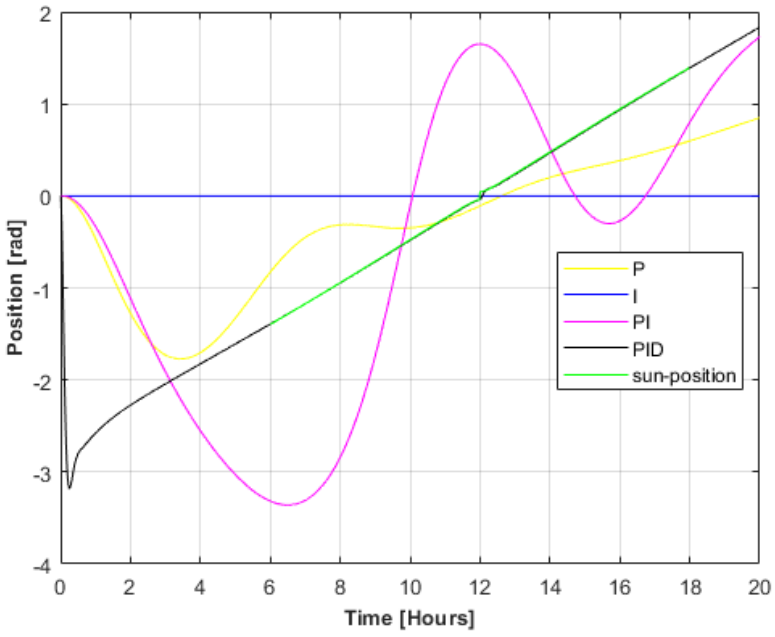

Figure 21. Controller comparison for nonlinear system in winter (day 173).

Similar to the responses in linearized model for winter, the PID is still the best controller as compared to other controllers. The fact that it works even for nonlinear model means it is worth considering. Comparison of the performance specifications with the controller integrated was made and the results are tabulated below.

Table 5. Comparison of the initial performance specification and PID controller performance specification

Specifications	Initially stated value	PID controller values
Maximum overshoot	20%	16.2%
Peak time	< 2 s	1.16 s
Settling time	< 3 s	0.854 s
Rise time	$<$ 0.3 s	0.105 s
Gain Margin	≥ 6 dB	39.8 dB
Phase Margin	$\geq 30°$	55.8°

7 DISCUSSIONS

The previous section looked at control tuning and/or design. PID was chosen and this was especially because of the way in which it responds to the input (sun's position). Performance specifications were outlined earlier on in section 2 where the desired performance specified in both time and frequency domains.

Settling time, which refers to the time it takes for the output of a system to reach and stay within a specific range of the final value after a sudden change in input, was observed. In this case a unit step input was introduced to see how the controlled plant would respond. Initially, the specified settling time of less than 3 seconds was desired, and the implementation of the controller resulted in settling time of 0.854 seconds. This means when the panel is disturbed during the sun path tracking process, it will take up to 0.854 seconds to get back to track. This value presents a percentage difference of about 71.53%.

Percentage overshoot, which refers to the temporary excursion of the output beyond its final, steady-state value after a sudden change in input, was also observed. The specified percentage overshoot was of value less than 20%. The implementation of controller resulted in percentage overshoot of about 16.2%. This means the panel would not oscillate forever when disturbance if exerted on it. From the specified value, the obtained value presents a percentage difference of about 19% which is not huge and creates room for improvement.

Peak time refers to the time it takes for the output of a system to reach its first maximum value after a sudden change in input was also considered. Initially, it was desired that this time should not surpass 2 seconds which was a success with control implementation. A peak time of 1.16 seconds was achieved which presents a percentage difference of about 43.16%.

The rise time was determined to be 0.105 seconds which is much lower than the initially required time of 0.3 seconds. This shorter rise time indicates faster system response, and it is no surprise that the percentage overshoot was at seen previously.

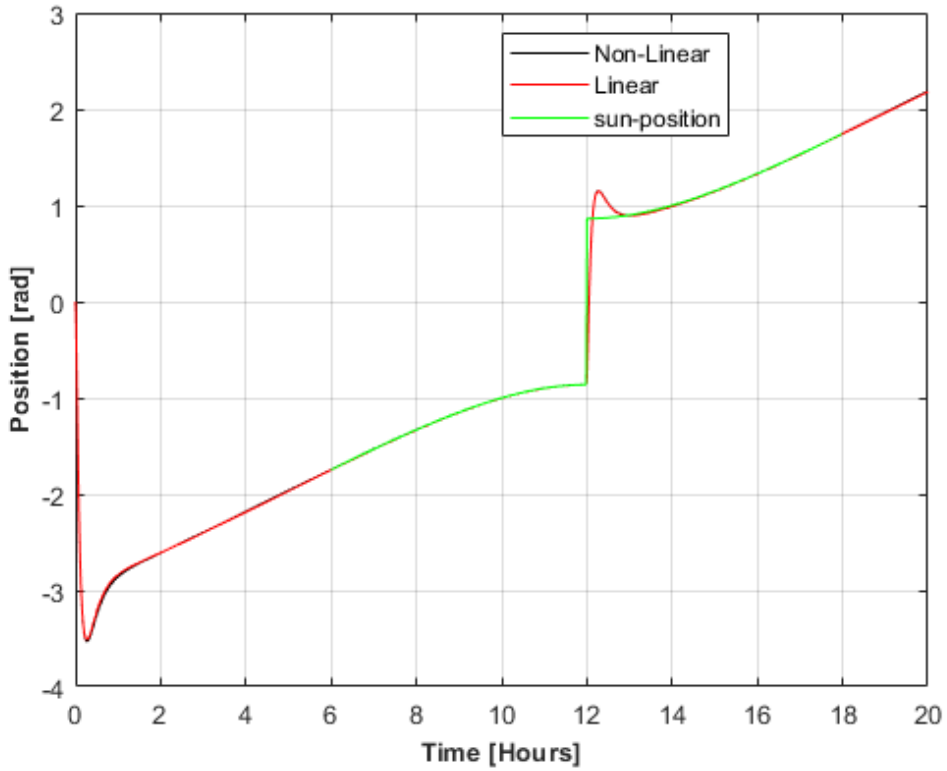

Figure 22. PID controlled response of linear and nonlinear compare with sun's position in summer.

The closed loop block diagram can be seen in the figure below. Since the method used did not specify the amount of gain for the system, the Routh Hurwitz method is used to determine the range of gain (K) for which the system is stable.

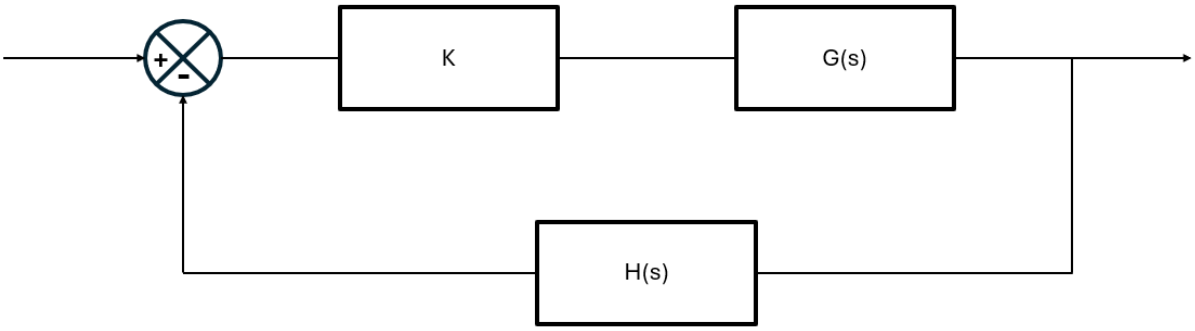

Figure 23 Closed loop block diagram.

For simplicity, the unity feedback was assumed. The new transfer function, accounting for the gain and the feedback loop is:

$$T(s) = \frac{KG(s)}{1 + KG(s)} \tag{7.1}$$

$$T(s) = \frac{0.0568K}{s^3 + 10.568s^2 + 11.278s + (55.682 + 0.0568K)} \tag{7.2}$$

The characteristic equation is:

$$s^3 + 10.568s^2 + 11.278s + (55.682 + 0.0568K) = 0 \tag{7.3}$$

For the equation to have the same sign throughout,

$$55.682 > -0.0568K$$

Solving this equation for K,

$$K > -980$$

The Routh array is now constructed,

Table 6 Routh Array for the closed loop system.

s^3	1	11.278
s^2	10.568	55.682 + 0.0568K
s^1	$\frac{-0.0568K + 63.504}{10.568}$	0
s^0	55.682 + 0.0568K	0

For the system to be stable,

$$\frac{-0.0568K + 63.504}{10.568} > 0$$

$$K < 1118$$

The overall range is given as,

$$-980 < K < 1118$$

8 CONCLUSION

This report details the design, modeling, and performance analysis of a solar tracking system for a 90m high building in Johannesburg, South Africa, equipped with Cinco 100W solar panels. The goal was to maximize solar energy capture amidst daily power cut-offs due to the country's power generation difficulties. The report comprehensively covers the system modeling, performance specifications, stability analysis, and controller design, concluding with the efficacy of the PID controller in maintaining optimal performance.

The solar tracking system was modeled using both linear and nonlinear approaches, considering the aerodynamic forces from the prevailing northerly winds. Assumptions included a 1:1 gear ratio and linearization of the nonlinear sine term in the equations of motion using small angle approximation.

Uncontrolled Plant Analysis:

- Simulations showed significant discrepancies between the linear and nonlinear models under various inputs (step, ramp, sine wave).
- The nonlinear model demonstrated more chaotic behavior, emphasizing the need for an effective control system.

Stability Analysis:

- The linear model was tested for stability using Routh-Hurwitz criterion, Nyquist plot, and pole-zero mapping. The system was found to be stable.
- The nonlinear model demonstrated BIBO stability, indicating that bounded inputs produce bounded outputs.

Closed-Loop Controller Design:

- The root locus method and PID control were employed to design a controller that aligns the panel's movement with the sun's trajectory.
- The PID controller was found to be the most effective in tracking the sun's position, outperforming P, I, and PI controllers in both summer and winter conditions.
- Performance with the PID controller showed improvements across all specifications: maximum overshoot (16.2%), peak time (1.16s), settling time (0.854s), and rise time (0.105s).

Comparison of Controlled vs. Uncontrolled Systems:

- The PID-controlled system significantly improved the solar panel's response time and accuracy in tracking the sun, ensuring higher efficiency in energy capture.
- Stability analysis of the closed-loop system using Routh-Hurwitz method determined the stable gain range to be $-980 < K < 1118$, confirming robustness against parameter variations.

The design and implementation of the PID controller for the solar tracker system successfully met the performance specifications and stability requirements. The controlled system demonstrated a marked improvement in response times and accuracy in aligning with the sun's position, ensuring enhanced energy efficiency. The robustness of the system against disturbances and variations in parameters further validates the effectiveness of the chosen control strategy.

9 REFERENCES

[1] SegenSolar, “Cinco,” 2 May 2024. [Online]. Available: https://segensolar.co.za/cinco-solar/.

[2] Communica, 2 May 2024. [Online]. Available: https://www.communica.co.za/products/solar-panel-cinco-100w.

[3] Global Forecast System, 10 May 2024. [Online]. Available: https://afriwx.co.za/wind/GFS-surface-wind-south-africa.php.

[4] G. S, The Anatomy of the Airfoil, Florida: Butterwoth Heineman, 2014.

[5] H. Y. Horng, Design of the Second-Order Controller by Time-Domain Objective Functions Using Cuckoo Search, London: Intechopen, 2019.

[6] N. S. Nise, Control Systems Engineering, Pomona: Wiley, 2019.

[7] N. Academy, Composer, *Introduction to Stability Analysis.* [Sound Recording]. 2022.

[8] P. A, “MECN4029A,” University of Witwatersrand, Johannesburg, 2024.

[9] N. S. Nise, Control Systems Engineering, California: Wiley.

10 APPENDICES

10.1 Appendix A: BIBO NonLinear stability Code

```
function dxdt = nonlinear_system(t, x)
    % Define the system of first-order differential equations
    dxdt = zeros(2,1);
    dxdt(1) = x(2);
    dxdt(2) = (2.78 - 5 * x(2) - 4.9 * sin(x(1))) / 1.2;
end

% Time span for the simulation
t_span = [0 10];

% Initial conditions for x(0) and dx/dt(0)
x0 = [0; 0];  % Initial conditions [x1(0); x2(0)]

% Solve the differential equation using ode45
[t, x] = ode45(@nonlinear_system, t_span, x0);

% Plot the results
figure;
plot(t, x(:,1), 'b', 'DisplayName', 'x(t)');
hold on;
plot(t, x(:,2), 'r', 'DisplayName', 'dx/dt(t)');
title('System Response to Bounded Input');
xlabel('Time (s)');
ylabel('State Variables');
legend('show');
grid on;

% Check if the output is bounded
is_bounded = all(abs(x(:,1)) < 10) && all(abs(x(:,2)) < 10); % Check if both
states remain within a reasonable bound
if is_bounded
    disp('The system is BIBO stable.');
else
    disp('The system is not BIBO stable.');
end
```

10.2 Appendix B: Stability Plots

```
% Define the polynomial coefficients
num = 0.0568;  % Numerator coefficient
den = [1, 10.568, 11.278, 55.682];  % Denominator coefficients

% Determine the roots of the polynomial
roots_den = roots(den);

% Display the roots
disp('Roots of the polynomial:');
disp(roots_den);
```

```
% Create the transfer function
sys = tf(num, den);

% Generate and display the pole-zero map
figure;
pzmap(sys);
title('Pole-Zero Map');

% Generate and display the Nyquist plot
figure;
nyquist(sys);
title('Nyquist Plot');

% Generate and display the Bode plot
figure;
bode(sys);
title('Bode Plot');
```

UNIVERSITY OF THE WITWATERSRAND, JOHANNESBURG

SCHOOL OF MECHANICAL, INDUSTRIAL & AERONAUTICAL ENGINEERING

Disclosure – Use of Artificial-Intelligence (AI) Generated Content

2024 V2

Students must acknowledge all use of AI.

Select all applicable statements and complete the sections fully. Delete all statements that are not applicable.

1. Disclosure: No AI use

☐ I acknowledge that no AI tools/technologies (Grammarly, ChatGPT, Bard, Quillbot, OpenAI etc) were used in the completion of this assessment.

2. Disclosure: Editing/refining grammar, spelling, formatting

☒ I acknowledge the use of XYZ, version, Month, Year (web url) to improve the explain what was edited/refined. I uploaded the text for my title of the assessment, and I entered the following prompts on Date, Month, Year:

Original prompt: " Paste the prompt"
User
A solar tracker controller for solar panel was designed for students to charge their devices during power cuts. To fully design this, different components of the system were considered. The main components were the motor and the panel which were mathematically modelled. Having considered the use of the power system required, performance specifications were outlined and formed a reference frame for the control design.
Performance analysis was done on uncontrolled system and from the behavior of the system, it was evident that control was necessary. Even though signs of stability from the uncontrolled were shown with the Routh Hurwitz method, this did not mean that control was not necessary. The system may be stable and still fail to meet the required performance, hence further analysis was undertaken to get a closed loop system. With a closed loop system, the output can be analyzed to see if it matches what the input is.
Further analysis was done to fully design the control for the system which ensured that the performance specifications are met. This was done by considering all the possible controllers that can be used. As mentioned earlier, PI controller was expected to be sufficient since the sun does not change its position fast. However, the design of a controller depends on a lot of factors and a controller cannot immediately be disregarded. PID controller was the selected controller for the solar tracker due to its impressive capability of following the sun's position as shown in the figure below.

fix the grammar and give flow and write this executing summary including the obtained transfer function, the gain range.
Follow-up prompt: " Paste the prompt"

The output from these prompts was used to state what action was made using the output.

3. Disclosure: Generated/manipulated text – list each occurrence

☐ I acknowledge the use of XYZ, version, Month, Year (web url) to explain what you used AI for. I entered the following prompt on Date, Month, Year:

"Paste the prompt"

The output from these prompts was used as explain where the output was used.

4. Disclosure: Generated/manipulated image – list each occurrence

☐ I acknowledge the use of XYZ, version, Month, Year (web url) to explain what you used AI for. I entered the following prompt on Date, Month, Year:

" Paste the prompt"

The output from these prompts was used as explain what the image was used for.

5. Disclosure: Generated/manipulated code – list each occurrence

☒ I acknowledge the use of XYZ, version, Month, Year (web url) to explain what you used AI for. I entered the following prompt on Date, Month, Year:

" Paste the prompt"
A polynomial is 0.0568/s^3+10.568s^2+11.278s+55.682

find a matlab code that determines the roots
the pole zero map
the nyquist criterion
the bode plot
then perform RH criteria

The output from these prompts was used as explain what the code was used for.

☒ ***I declare that the disclosure is complete and truthful.***

Student number: 2350229
Course code: MECN4029
Date:20 May 2024